J Mol Model (2015) 21: 10
DOI 10.1007/s00894-014-2559-z

ORIGINAL PAPER

Theoretical studies of the nitrogen containing compounds adsorption behavior on Na(I)Y and rare earth exchanged RE(III) Y zeolites

Wei Geng · Haitao Zhang · Xuefei Zhao · Wenyan Zan · Xionghou Gao · Xiaojun Yao

Received: 2 April 2014 / Accepted: 7 December 2014 / Published online: 22 January 2015

Abstract In this work, the adsorption behavior of nitrogen containing compounds including NH_3, pyridine, quinoline, and carbazole on Na(I)Y and rare earth exchanged La(III)Y, Pr(III)Y, Nd(III)Y zeolites was investigated by density functional theory (DFT) calculations. The calculation results demonstrate that rare earth exchanged zeolites have stronger adsorption ability for nitrogen containing compounds than Na(I)Y. Rare earth exchanged zeolites exhibit strongest interaction with quinoline while weakest with carbazole. Nd(III)Y zeolites are found to have strongest adsorption to all the studied nitrogen containing compounds. The analysis of the electronic total charge density and electron orbital overlaps show that nitrogen containing compounds interact with zeolites by π-electrons of the compounds and the exchanged metal atom. Mulliken charge population analysis also proves that adsorption energies are strongly dependent on the charge transfer between the nitrogen containing molecules and exchanged metal atom in the zeolites.

Keywords Charge transfer · Density functional theory · Denitrogasenation · Rare earth · Zeolites

W. Geng · X. Zhao · W. Zan · X. Yao (✉)
Department of Chemistry, Lanzhou University, Lanzhou 730000, China
e-mail: xjyao@lzu.edu.dn

H. Zhang · X. Gao (✉)
Petrochemical Research Institute, Lanzhou Petrochemical Research Center, PetroChina Company Limited, Lanzhou 730060, China
e-mail: gaoxionghou@petrochina.com.cn

X. Gao
e-mail: xionghougao@163.com

Introduction

Deep denitrogenation of fossil fuels, such as crude petroleum oil, has drawn extensive attention in the industrial sector during recent years [1–3]. Nitrogen-containing compounds in fuels remain a major source of air pollution and have many negative effects on the environment [4]. For instance, nitrogen-containing compounds are one of the main reasons for the heavy haze days in Eastern China [5]. Direct combustion of nitrogen-containing compounds presented in the fuel also leads to NO_x emission, which is harmful to human health and results in acid mist and acid rain. In order to comply with the tightening environmental regulation, denitrogenation of fossil fuels become one of the most crucial tasks of modern petroleum refinery. On the other hand, because of the ongoing consumption of fuels from limited natural resources, petroleum refineries must treat a lot of heavy low-quality crude oil, which is rich in highly refractory nitrogen containing compounds.

Conventional hydrotreating methods have been effective due to easy-to-remove sulfur and nitrogen containing compounds, while less competent for removing heterocyclic sulfur or nitrogen containing compounds which are abundant especially in diesel. In the catalytic hydrotreating process, denitrogenation (HDN) and desulfurization (HDS) are performed simultaneously. The ability to absorb aromatic thiophene derivatives is generally competing with nitrogen compounds during hydrotreating processes [6]. Although nitrogen concentration in diesel fuel is usually much lower than the sulfur concentration, HDN is still the most difficult hydrotreatment reaction and much slower than HDS. In addition, nitrogen containing compounds coexist in middle-distillate oil and NH_3 produced during the hydrocarbon reforming process are poisonous to the catalysts. Therefore, it is necessary and important to develop new approaches to ultra-deep desulfurization and denitrogenation for diesel fuels.

As an alternative method to conventional hydrotreating methods, selective adsorption methods appear to be very promising for ultra-deep desulfurization and denitrogenation at ambient temperature and pressure without consuming pressurized hydrogen or oxygen gas, which may finally lead to major advances in petroleum refining [7–14]. In addition, adsorbents can be regenerated by using proper methods. However, for selective adsorption to be viable, an effective adsorbent that can selectively adsorb sulfur and nitrogen containing compounds must be developed. Silicon-based adsorbent has been proved to be a high selectivity of nitrogen-containing compounds at mild temperature and ambient pressure [9]. Kwon et al. designed mesoporous silica adsorbents with Zr ions and could contribute to the production of clean fuels through preferential adsorption of nitrogen- and sulfur-containing compounds from light gas oil and heavy catalytic naphtha in refinery streams [3]. Lithium-modified mesoporous silica adsorbents (YSP-Li and MCF-Li) were prepared to selectively remove nitrogen compounds from residue hydrodesulfurization diesel and exhibited improved performance both in adsorption capacity and the adsorption rate [10]. Furthermore, Li-modified adsorbents could be easily regenerated by methyl isobutyl ketone (MIBK) [10]. Yang and his co-workers also reported that Cu(I)Y was an effective adsorbent and capable of being used both in deep desulfurization and denitrogenation with high selectivity and high capacity [7].

In our previous work, we have theoretically studied the interaction between rare earth exchange Y zeolite (RE(III)Y) and thiophenic compounds by using first principle calculations based on density functional theory (DFT) [15]. It was found that π-electrons complexation dominated the interaction between RE(III)Y and thiophenic sulfur compounds. The adsorption energies are closely related to the charge transfer between small molecules and zeolites. Inspired by the success in previous experimental works on simultaneous desulfurization and denitrogenation, we here investigated the possible adsorption capability of nitrogen-contained molecules on three rare earth exchanged Y type zeolites as well as and the detailed interaction mechanism between them. RE exchanged zeolites were often prepared by ion exchange with Na(I)Y zeolite in industrial and the products usually contained residual Na^+ ions. Therefore, we also calculated the adsorption behavior of nitrogen containing compounds on Na(I)Y as a comparison. As we know, little has been reported on denitrogenation in transportation fuels use rare earth exchanged Y type zeolites. In this work, we investigated the adsorption of nitrogen-containing molecules including NH_3, pyridine, quinoline, and carbazole on Na(I)Y and rare earth exchanged La(III)Y, Pr(III)Y, Nd(III)Y zeolites using DFT method. The adsorption configurations and details about charge transfer were also calculated. The results of our study could lead to a better understanding about the adsorption mechanisms in deep denitrogenation of gasoline and diesel fuels and guide the manufacture of industrial products.

Computational details

In Y zeolite, extra-framework cations are located at several crystallographic sites [16]. Site II in the supercage coordinates with three oxygen atoms of the six-ring window of the sodalite cage and is the active sites for those adsorbed molecules. In addition, Monte Carlo simulation based on the Adsorption Locater module in Materials Studio 5.5 software package (Accelrys Ltd., USA) also demonstrates that cations are mostly located in site II [17]. In order to consider the influence of zeolite framework and pore on adsorption behavior, we employed the widely used finite cluster. A 12 T (T=tetrahedral unit of zeolite) cluster with six-membered ring and six other Si atoms of the partial of supercage was cut from the framework of the FAU zeolite. The dangling bonds of oxygen atoms located at the cluster edge were saturated by hydrogen atoms directed along the bond vector of what would have been the next zeolite framework atom in the crystal structure. The terminal OH bonds were set to be 1.0 Å. The positions of the terminal OH groups were fixed during geometry optimizations, whereas all the other atoms were allowed to relax. For cation-exchanged zeolites, to stabilize the exchanged cation, the Na(I)Y ($NaAlSi_{11}O_{33}H_{18}$) cluster model should have one Al atom to maintain the system neutral. In the same way, La(III)Y, Pr(III)Y, and Nd(III)Y ($REAl_3Si_9O_{33}H_{18}$) should also have three Al atoms, respectively, which substituted three Si atoms of the six-member ringed in an alternating sequence to following Loewenstein's rule [18] that two tetrahedrally coordinated aluminum atoms cannot share an oxygen atom.

All the DFT calculations were performed by Dmol3 program in Materials Studio 5.5 package. The generalized gradient approximation (GGA) with the Becke [19] gradient exchange functional and Lee–Yang–Parr [20] correlation functional (BLYP) were used to treat all electronic energy of exchange correlation. Double-numeric quality base set with the polarization functions (DNP) [21] was employed, which is comparable with the Gaussian 6-31G** basis set in size and quality. The core electrons were treated with DFT semicorepseudo potentials (DSPPs). In a previous work, Inana et al. [22] confirmed that the magnitude of basis set superposition error (BSSE) in the numerical basis set in $DMol^3$ is very small. $DMol^3$ uses exact DFT spherical-atomic orbitals that are generated numerically. The molecule can be dissociated exactly into their constituent atoms within the DFT context, indicating the nearly perfect basis set for the separated atoms limit. Thus we do not consider the BSSE. A thermal smearing of 0.005 Ha and an orbital cut-off of 5.8 Å was used to improve the computational performance. The convergence criteria for the geometry optimization and energy calculation

were set as follows: (a) an energy tolerance of 1.0 E-5Ha, (b) a maximum force tolerance of 0.002 Ha/Å, and (c) a maximum displacement tolerance of 0.005 Å. The adsorption energies were calculated by using the expression:

$$E_{Ads} = E_{N/zeolite} - E_N - E_{zeolite},$$

where $E_{N/zeolite}$ is the total energy of the optimized complex compounds of the nitrogen-containing compounds on the zeolite clusters, E_N is the energy of the nitrogen-containing compounds and $E_{zeolites}$ is the energy of the optimized zeolite clusters.

Results and discussion

Geometry of isolated nitrogen-containing molecules and zeolites

Before we calculated the adsorption systems, we performed DFT calculation for the isolated zeolite and nitrogen-containing molecules. The isolated NH_3, pyridine, quinoline, and carbazole as well as zeolite clusters were firstly optimized. The molecular structures and optimized geometries of pyridine, quinoline, and carbazole molecules as well as the optimized structures of Na(I)Y and La(III)Y clusters are given in Fig. 1. The 6-membered ring at the center of clusters is composed of six T atoms and six O atoms. These six O atoms are nearly coplanar, and we marked the centroid (X) of the six O atoms. To describe the distance between RE atoms and the Y zeolite more accurately, we calculated the distance between exchanged metal atoms (M) and centroid (X) mentioned above. Compared with Na(I)Y, La(III)Y exhibits higher symmetry as shown in Fig. 1e, and exhibits shorter distance between the La and the X, which means interaction between La and skeleton is stronger than that of Na. The configurations of Pr(III)Y and Nd(III)Y are similar to that of La(III)Y. As shown in Table 1, the distances between RE atoms to the X are all shorter than that of Na, in the order of Nd(III)Y< Pr(III)Y<La(III)Y.

NH_3 adsorption on zeolites

NH_3 was produced during the hydrocarbon reforming process, and it was also used as a probe molecule to investigate the acid of the active site in zeolite [23, 24]. We firstly studied NH_3 adsorption behavior on zeolites. NH_3 molecule was placed on the site with the N atom toward the RE or Na atoms. After full relaxation, the optimized geometries for NH_3 adsorption on the Na(I)Y and La(III)Y are shown in Fig. 2a and b. The distances between atoms in NH_3 and zeolites are listed in Table 1, which can help to learn more details about the interaction mechanism. For NH_3 on Na(I)Y, the distance between N atom and Na atom was 2.44 Å. After NH_3 absorption on Na(I)Y, Na^+ moved away from zeolite framework, the distance of X-M was 1.09 Å. Compared with the isolated Na(I)Y, this distance increased 0.27 Å. Adsorption energy of NH_3 adsorbed on Na(I)Y is −75.33 kJ mol^{-1}.

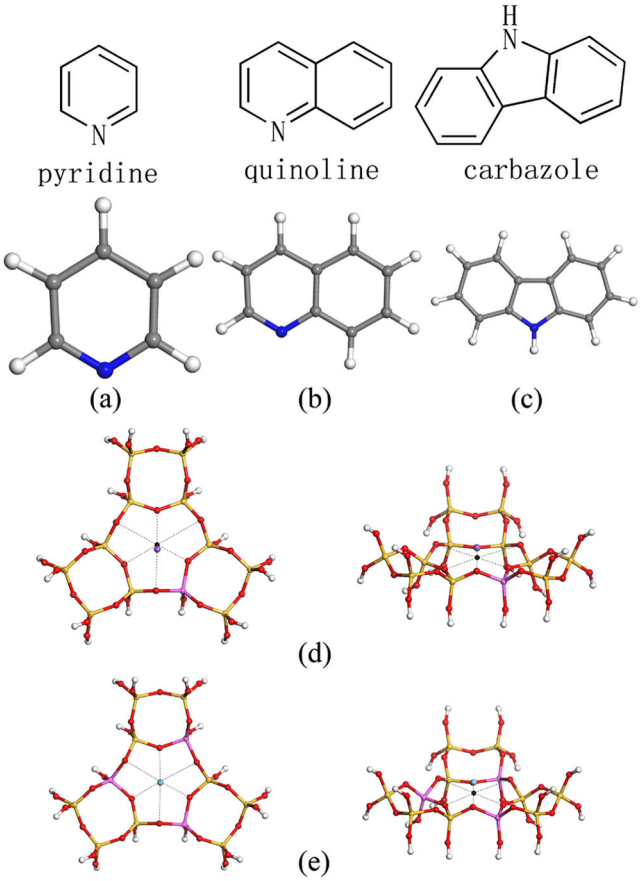

Fig. 1 The molecular structures and optimized geometries of (**a**) pyridine, **b** quinoline, **c** carbazole, and optimized structures of (**d**) Na(I)Y and (**e**) La(III)Y clusters

For NH_3 adsorbed on RE(III)Y, the N-M distance of RE(III)Y are all longer than that of Na(I)Y. However, it did not mean the molecule was far away from the zeolite, the distances between N atoms and centroid X of zeolites were shorter compared to that of Na(I)Y system. Compared with the distance before adsorption, the distances between exchanged RE atoms and centroid X increased no more than 0.06 Å, which were far less than that of Na(I)Y, indicating the RE(III) exchanged atoms were more stable at the exchanged site. The distances of N-M, N-X, and M-X for NH_3 adsorbed on RE(III)Y were all in the order of Nd(III)Y<Pr(III)Y<La(III)Y. Adsorption energies of NH_3 adsorbed on RE(III)Y were nearly twice as that of Na(I)Y. Nd(III)Y showed the highest adsorption energy of −135.43 kJ mol^{-1}. RE(III)Y showed stronger acid than Na(I)Y and the RE atoms played a key role in the interaction.

Table 1 Distances (Å) of isolated zeolites and absorption systems

	Iso	NH_3			Pyridine			Quinoline			Carbazole		
	M-X	N-M	N-X	M-X	N-M	N-X	M-X	N-M	N-X	M-X	N-M	N-X	M-X
Na(I)Y	0.82	2.44	3.44	1.09	2.43	3.43	1.02	2.44	3.47	1.06	3.73	4.44	1.16
La(III)Y	0.76	2.77	3.43	0.81	2.70	3.47	0.80	2.66	3.43	0.77	3.38	4.08	0.89
Pr(III)Y	0.61	2.69	3.26	0.66	2.61	3.25	0.64	2.61	3.27	0.66	3.18	3.83	0.77
Nd(III)Y	0.61	2.66	3.19	0.59	2.58	3.20	0.62	2.60	3.24	0.65	3.78	4.34	0.75

Pyridine and quinoline adsorption on zeolites

Six-membered nitrogen heterocyclic were basic species in petroleum oil [25–27]. Two typical basic nitrogen compounds, pyridine and quinoline were investigated here. To investigate the favorable adsorption configuration, we used two different initial states, in one the molecules lie on the modified atoms and in the other the molecules stand with N toward metal atom. For the first situation, even if the pyridine and quinoline were placed in parallel conformations, after relaxation, the nitrogen containing molecules turned to standup conformations with N atoms toward the metal cation. The optimized geometrical structures were similar for the two initial structures. The most energetically stable optimized geometrical structures for the pyridine and quinoline adsorption on Na(I)Y and La(III)Y are listed in Fig. 3. These conformations were quite different from that of thiophenic molecules adsorption on rare earth exchanged zeolites in our previous study [15]. The latter tend to form the conformation of thiophene molecules almost parallel on the absorption site. The pyridine and quinoline molecules interacted with modified metal atoms by direct N-metal bonds instead of S and π-electrons of heterocyclic interaction in the case of thiophene adsorption on Y zeolites. Configurations of pyridine and quinoline on the other RE(III)Y were similar to La(III)Y.

For pyridine and quinoline adsorption on Na(I)Y, the distances of N-M and N-X were nearly the same as NH_3 on Na(I)Y; the outside moves of Na were also observed. The adsorption energies were −65.09 and −62.15 kJ mol^{-1} respectively, which were lower than that of NH_3 on Na(I)Y about 10 kJ mol^{-1}. These results suggested the larger molecules may lead to the decrease of adsorption energy on Na(I)Y. In the actual oil, the existence of polycyclic molecules and its substituent homologue may result in lower adsorption performance of Na(I)Y. For pyridine and quinoline adsorption on RE(III)Y, as shown in Table 1, the distances of N-M, N-X and M-X were all in the order of Nd(III)Y< Pr(III)Y<La(III)Y, as RE atomic number increase, the distances tended to decrease. Compared with Na(I)Y, Pr(III)Y, and Nd(III)Y showed shorter N-X distance, which reflected the distance between molecules and zeolites framework. The same as that in the situation of NH_3

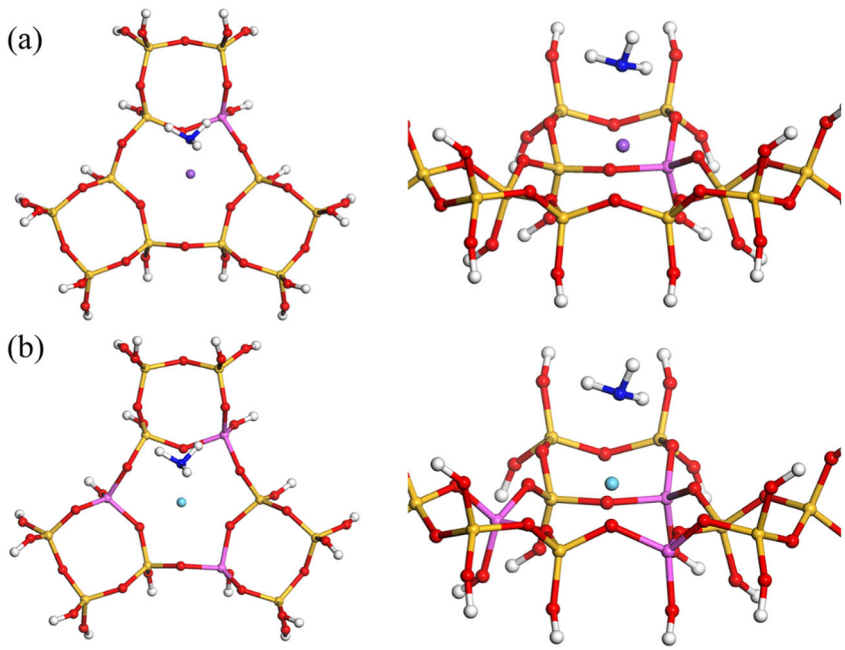

Fig. 2 Adsorption configurations of NH_3 on (**a**) Na(I)Y zeolites (**b**) La(III)Y zeolites. Left is top views and right is side views

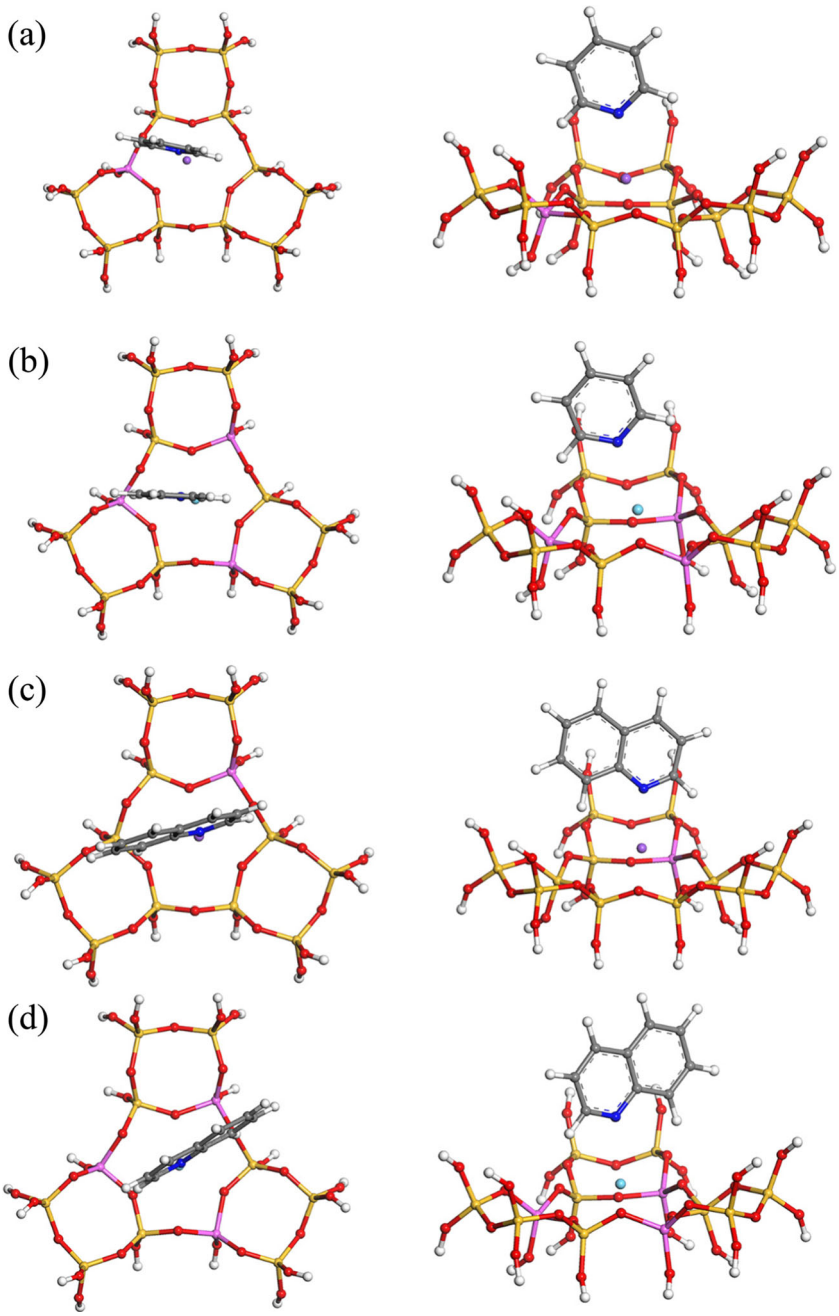

Fig. 3 Adsorption configurations of (**a**) pyridine on Na(I)Y, (**b**) pyridine on La(III)Y, (**c**) quinoline on Na(I)Y, (**d**) quinoline on La(III)Y. Left is top views and right is side views

absorption, RE(III) atoms were hardly moved outside. The adsorption energies of pyridine and quinoline adsorption on RE(III)Y were ranging from −127.91 to −146.42 kJ mol^{-1}, which were nearly twice that of Na(I)Y. Among the three RE(III)Y, the adsorption of Nd(III)Y was strongest and Pr(III)Y was weakest for pyridine and quinoline adsorption. Moreover, although the adsorbed molecules became larger, adsorption energies do not decreased like Na(I)Y, even increase for Pr(III)Y and Nd(III)Y. The improved performance indicates RE exchanged zeolite was energetically favorable for adsorption of basic N-heterocyclic molecules in petroleum oil.

To look at insight into the electronic interactions between pyridine, quinoline, and RE(III)Y zeolites, we also calculated the electronic total charge density and Mulliken charge populations [28] for the pyridine, quinoline adsorbed on RE(III)Y systems. Electronic total charge density plots with color mapped iso-surfaces of pyridine and quinoline on Na(I)Y and La(III)Y are given in Fig. 4. As shown in Fig. 4, it is obvious the electron cloud overlaps locate between N atom of pyridine, quinoline and exchanged metal atoms. On the edge of pyridine, quinoline molecules, electron cloud hardly overlaps with zeolites. The color of the electron cloud demonstrated the iso-surfaces values. The minimum value of iso-surfaces

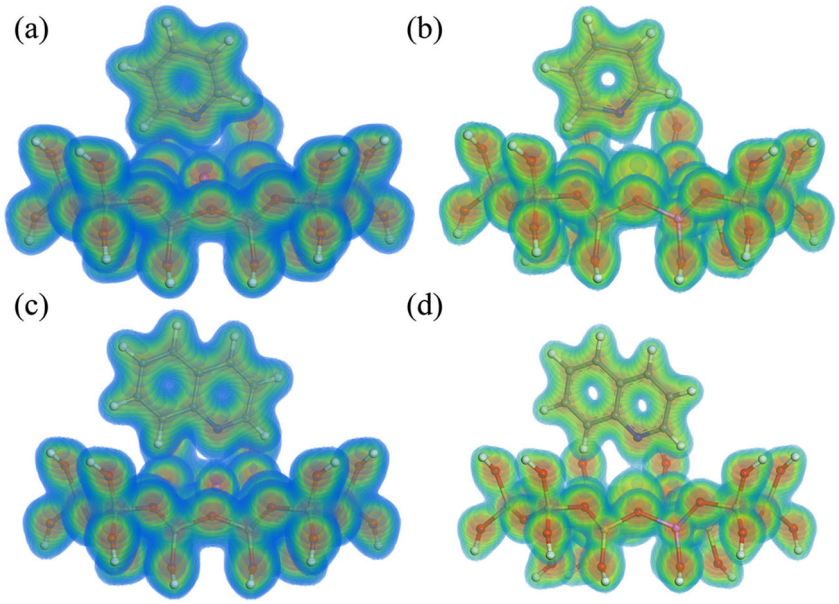

Fig. 4 Electronic total charge densities for (**a**) pyridine on Na(I)Y, **b** pyridine on La(III)Y, **c** quinoline on Na(I)Y, **d** quinoline on La(III)Y. The minimum values of iso-surface are 0.13 e/Å^3 for Na(I)Y and 0.26 e/Å^3 for La(III)Y systems respectively

were 0.13 e/Å^3 for Na(I)Y and 0.26 e/Å^3 for La(III)Y systems respectively. Electron orbital overlaps between pyridine, quinoline, and Na(I)Y were relative weaker, while those on La(III)Y exhibit stronger overlaps with values about double. To further understand the charge transfer of pyridine, quinoline on Na(I)Y and RE(III)Y, Mulliken charge populations were calculated. Before pyridine and quinoline adsorption, Mulliken charge populations for Na, La, Pr, and Nd atoms were 0.73, 1.45, 1.17, and 1.16 respectively. The positive charges for all of the metal atoms suggested a part of the electrons of metal atoms transfer to zeolite framework atoms. Exchanged metal atoms as a Lewis acid could provide an empty orbital to accept electrons from alkali such as the N atom of pyridine, quinoline. The populations of RE(III) atoms are more positive than Na which indicated more electrons of RE atoms transferred to zeolite framework. For molecular adsorption systems, Δe_N is charge transfer from pyridine or quinoline to zeolite; Δe_M is the difference between charge population of exchanged metal atom after and before molecular adsorption. As Tables 2 and 3 show, in the case of pyridine or quinoline absorbed on Na(I)Y, both Δe_N are 0.06e and Δe_M are −0.02, indicating that charge transfers are very weak. For pyridine adsorbed on La(III)Y, Pr(III)Y, and Nd(III)Y, Δe_N are 0.22, 0.28, and 0.28 respectively, and the Δe_M are all −0.08, which were 3~4 times than that of Na(I)Y. The charge transfer of quinoline on RE(III)Ys are even larger than pyridine. Furthermore, charge transfer of Pr(III)Y and Nd(III)Y were a little larger than La(III)Y. These trends are the same as the adsorption energies. The large charge transfers confirm that the pyridine, quinoline act as electron donors, and the RE atoms act as a Lewis acid site, there are strong Lewis acid-base interactions between them. It is noticed that the charge transfer of molecules are not equal to the metal, indicating a part of the electrons are transfered to zeolite framework. Compared to thiophenic molecules, pyridine and quinoline molecules are strong Lewis bases, the N atoms of the base site directly interact with the acid site of the metal cation. Since Mulliken atomic charges are dependent on the basis set and may lead to errors, we also calculated NBO charges and compared with Mulliken charges. For pyridine and quinoline on Na(I)Y, the Δe_N are 0.04 and 0.04; while on La(III)Y, the Δe_N are 0.11 and 0.13. These results also indicated that the charge transfer for La(III)Y system was about three times than

Table 2 Adsorption energies (kJ mol^{-1}) of nitrogen compounds adsorption on zeolites

	NH_3	Pyridine	Quinoline	Carbazole
Na(I)Y	−75.33	−65.09	−62.15	−30.16
La(III)Y	−132.94	−132.03	−132.92	−104.16
Pr(III)Y	−128.84	−132.83	−135.99	−99.23
Nd(III)Y	−135.43	−143.62	−146.42	−117.08

Table 3 The Mulliken charge populations of isolated zeolites and absorption systems

	$e_{M\ (isolated)}$	Pyridine		Quinoline		Carbazole	
		Δe_N	Δe_M	Δe_N	Δe_M	Δe_N	Δe_M
Na(I)Y	0.73	0.06	−0.02	0.06	−0.02	−0.01	0.02
La(III)Y	1.45	0.22	−0.08	0.26	−0.12	0.23	−0.09
Pr(III)Y	1.17	0.28	−0.08	0.31	−0.11	0.36	−0.08
Nd(III)Y	1.16	0.28	−0.08	0.31	−0.10	0.37	−0.09

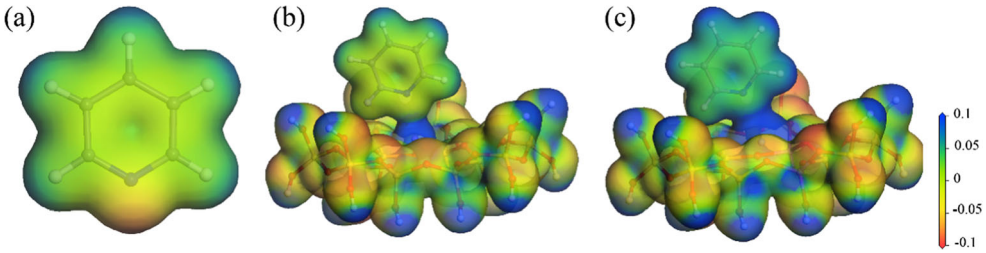

Fig. 5 Electrostatic potentials of (**a**) pyridine (**b**) pyridine on Na(I)Y, **c** pyridine on La(III)Y with an iso-surfaces of charge densities value of 0.05

that of Na(I)Y. In order to further demonstrate the charge transfer of the nitrogen-containing molecules, we calculated the electrostatic potentials of them before and after absorption as shown in Figs. 5 and 6. It is obvious that the regions around the N atom of isolated pyridine and quinolines show negative electrostatic potentials due to the lone pair electrons of the N atom. After sorption on the zeolites, the N atom bonds with the metal atom which exhibits strong positive electrostatic potential. The pyridine and quinoline molecules show blue color after absorption on the La(III)Y compared with isolated and on the Na(I)Y, indicating the large charge transfer from molecules to the La(III)Y zeolite.

Carbazole adsorption on zeolites

Five-membered nitrogen containing heterocyclic compounds were neutral species in petroleum oil [25–27]. We considered the adsorption of carbazole on Na(I)Y and RE(III)Y zeolites in our work. The same as that in the cases of pyridine and quinoline, we considered two different initial states: lie-down and stand-up. However, the results from carbazole were contrary to the pyridine and quinoline. The most energetically stable geometries for carbazole were lie-down conformations as shown in Fig. 7. In the basic heterocyclic nitrogen containing compounds with six-membered pyridine ring, two electrons were involved in C-N bond, one electron involved in conjugated large π bond, the rest of the lone pair electrons were located in the plane of the molecule and responsible for its Lewis basicity. In the neutral heterocyclic nitrogen containing compounds with five-membered pyrrole ring, three electrons were involved in one N-H bond and two C-N bonds on the plane of the molecule. The other two electrons were involved in a conjugated large π bond and were delocalized. Therefore, carbazole interacted with modified metal atoms by the π-electron and showed lie-down conformations.

For carbazole adsorption on Na(I)Y, the distance of N-M was 3.73 Å, clearly indicating there is no chemical bond between N and Na atoms. The distances of M-X were 1.16 Å, suggesting a more serious outside move of the Na atom. The adsorption energy was −30.16 kJ mol^{-1} only. For carbazole adsorption on RE(III)Y, although the adsorption energies somewhat decreased, it was still considerable, for the most energetic Nd(III)Y it reached −117.08 kJ mol^{-1}. RE(III)Y could effectively removed even the neutral nitrogen molecules compared with Na(I)Y. Figure 8 showed the electronic total charge density plots of carbazole on Na(I)Y and La(III)Y. The minimum value of iso-surfaces were 0.13 e/$Å^3$ for Na(I)Y and 0.26 e/$Å^3$ for La(III)Y systems respectively. As shown in Table 2, carbazole absorbed on Na(I)Y, both Δe_N were −0.01e and Δe_M were 0.02. Within the given method error bounds, there is hardly charge transfer between Na atom and the carbazole molecule. For carbazole adsorbed on La(III)Y, Pr(III)Y, and Nd(III)Y, Δe_N were ranged from 0.23 to 0.37 and the Δe_M were about −0.08. The modified RE atoms acted as an acid site. The NBO charge for carbazole on Na(I)Y and La(III)Y are also calculated, Δe_N were 0.03 and 0.15 respectively, the charge transfer on La(III)Y are larger than Na(I)Y, and the interaction between carbazole and La(III)Y are stronger. We also calculated the electrostatic potentials of carbazole absorption on the zeolites. As Fig. 9 shows, the N atom of isolated carbazole molecules show positive electrostatic potentials, which is different from pyridine and quinoline since the H atom connected with N of carbazole. After sorption on La(III)Y, carbazole molecules also become more blue colored compared with that on the Na(I)Y, it could be seen as the molecules are polarized by the La(III)Y zeolite [29].

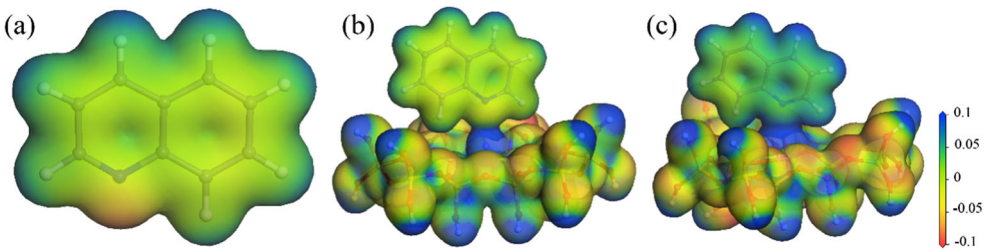

Fig. 6 Electrostatic potentials of (**a**) quinoline, **b** quinoline on Na(I)Y, **c** quinoline on La(III)Y with an iso-surfaces of charge densities value of 0.05

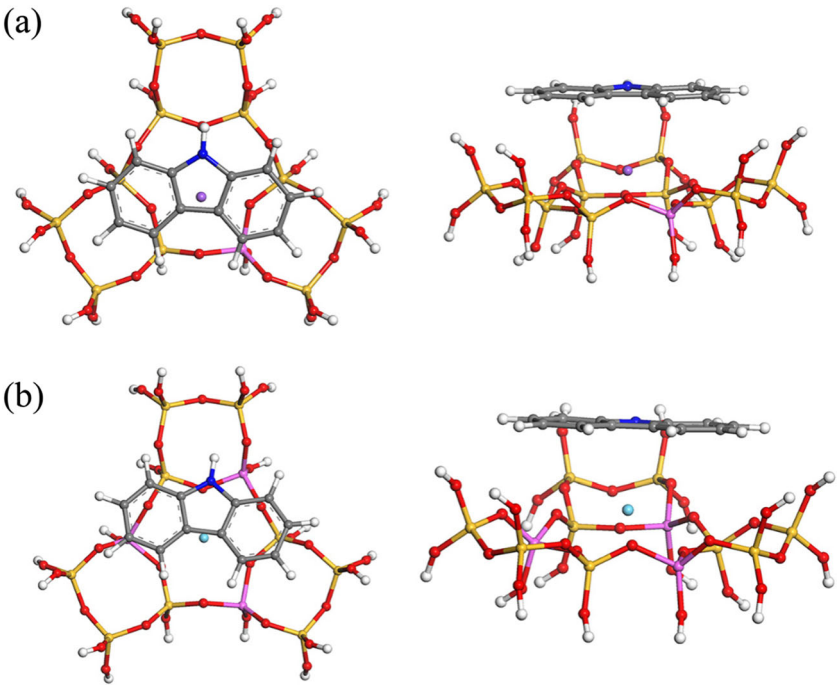

Fig. 7 Adsorption configurations of carbazole on (**a**) Na(I)Y, **b** La(III)Y. Left is top views and right is side views

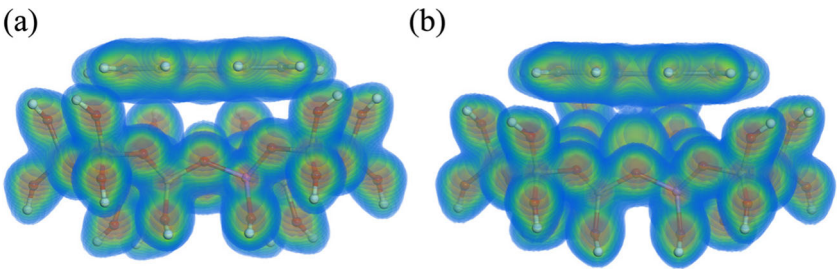

Fig. 8 Electronic total charge densities for carbazole on (**a**) Na(I)Y, **b** La(III)Y. The minimum value of iso-surfaces is 0.13 e/Å^3

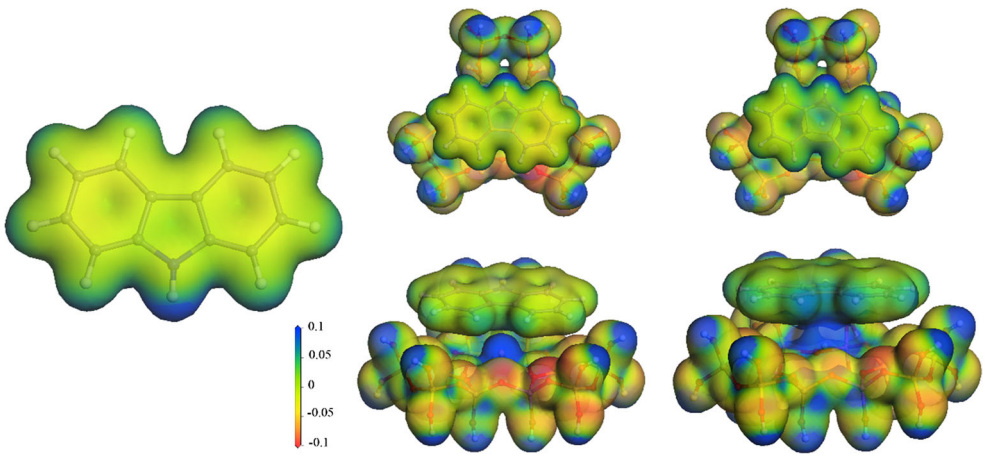

Fig. 9 Electrostatic potentials of (**a**) carbazole, **b** carbazole on Na(I)Y, **c** carbazole on La(III)Y with an iso-surfaces of charge densities value of 0.05

Conclusions

In summary, the adsorption behavior of NH_3, pyridine, quinoline, and carbazole on Na(I)Y and RE(III)Y zeolites were studied by DFT calculations. The calculation results demonstrate that RE(III)Y are promising absorbent for nitrogen containing compounds such as NH_3, pyridine, quinoline, and carbazole. The modified RE (III) atoms act as a strong acid site and play an important role in the adsorption. Further Mulliken charge population analysis also confirmed the importance of RE(III) in the adsorption. The results also proved that the studied basic organic molecules adopted stand-up configuration on the RE(III)Y and formed chemical bond; neutral organic adopted lie-down configuration on the RE(III)Y and interacted with modified metal atoms by π-electrons.

Acknowledgments This work was supported by PetroChina Company Limited (Grant No. 2010E-1901).

References

1. Kim JH, Ma X, Zhou A, Song C (2006) Ultra-deep desulfurization and denitrogenation of diesel fuel by selective adsorption over three different adsorbents: a study on adsorptive selectivity and mechanism. Catal Today 111:74–83
2. Zeuthen P, Knudsen KG, Whitehurst DD (2001) Organic nitrogen compounds in gas oil blends, their hydrotreated products and the importance to hydrotreatment. Catal Today 65:307–314
3. Kwon J-M, Moon J-H, Bae Y-S, Lee D-G, Sohn H-C, Lee C-H (2008) Adsorptive desulfurization and denitrogenation of refinery fuels using mesoporous silica adsorbents. ChemSusChem 1:307–309
4. Aneja VP, Roelle PA, Murray GC et al (2001) Atmospheric nitrogen compounds II: emissions, transport, transformation, deposition and assessment. Atmos Environ 35:1903–1911
5. Zhao XJ, Zhao PS, Xu J et al (2013) Analysis of a winter regional haze event and its formation mechanism in the North China Plain. Atmos Chem Phys 13:5685–5696
6. Sumbogo Murti SD, Yang H, Choi K-H, Korai Y, Mochida I (2003) Influences of nitrogen species on the hydrodesulfurization reactivity of a gas oil over sulfide catalysts of variable activity. Appl Catal A Gen 252:331–346
7. Hernández-Maldonado AJ, Yang RT (2004) Denitrogenation of transportation fuels by zeolites at ambient temperature and pressure. Angew Chem Int Ed 43:1004–1006
8. Liu D, Gui J, Sun Z (2008) Adsorption structures of heterocyclic nitrogen compounds over Cu(I)Y zeolite: a first principle study on mechanism of the denitrogenation and the effect of nitrogen compounds on adsorptive desulfurization. J Mol Catal A Chem 291:17–21
9. Shiraishi Y, Yamada A, Hirai T (2004) Desulfurization and denitrogenation of light oils by methyl viologen-modified aluminosilicate adsorbent. Energy Fuel 18:1400–1404
10. Koriakin A, Ponvel KM, Lee C-H (2010) Denitrogenation of raw diesel fuel by lithium-modified mesoporous silica. Chem Eng J 162: 649–655
11. Bae Y-S, Kim M-B, Lee H-J, Lee C-H, Wook RJ (2006) Adsorptive denitrogenation of light gas oil by silica-zirconia cogel. AIChE J 52: 510–521
12. Laredo GC, Vega-Merino PM, Trejo-Zárraga F, Castillo J (2013) Denitrogenation of middle distillates using adsorbent materials towards ULSD production: a review. Fuel Process Technol 106:21–32
13. Sano Y, Choi K-H, Korai Y, Mochida I (2004) Adsorptive removal of sulfur and nitrogen species from a straight run gas oil over activated carbons for its deep hydrodesulfurization. Appl Catal B Environ 49: 219–225
14. Xie L-L, Favre-Reguillon A, Wang X-X, Fu X, Lemaire M (2010) Selective adsorption of neutral nitrogen compounds from fuel using ion-exchange resins. J Chem Eng Data 55:4849–4853
15. Gao X, Geng W, Zhang H, Zhao X, Yao X (2013) Thiophenic compounds adsorption on Na(I)Y and rare earth exchanged Y zeolites: a density functional theory study. J Mol Model 19:4789–4795
16. Frising T, Leflaive P (2008) Extraframework cation distributions in X and Y faujasite zeolites: a review. Microporous Mesoporous Mater 114:27–63
17. Sung C-Y, Al Hashimi S, McCormick A, Tsapatsis M, Cococcioni M (2011) Density functional theory study on the adsorption of H2S and other Claus process tail gas components on copper- and silver-exchanged Y zeolites. J Phys Chem C 116:3561–3575
18. Jentys A, Lercher JA (2001) Techniques of zeolite characterization, Chap 8. In: van Bekkum H, Flanigen EM, Jacobs PA, Jansen JC (eds) Studies in surface science and catalysis. Elsevier, Amsterdam, pp 345–386
19. Becke AD (1993) Density-functional thermochemistry. III. The role of exact exchange. J Chem Phys 98:5648–5652
20. Lee C, Yang W, Parr RG (1988) Development of the Colle-Salvetti correlation-energy formula into a functional of the electron density. Phys Rev B 37:785–789
21. Delley B (2000) From molecules to solids with the DMol3 approach. J Chem Phys 113:7756–7764
22. Inada Y, Orita H (2008) Efficiency of numerical basis sets for predicting the binding energies of hydrogen bonded complexes: evidence of small basis set superposition error compared to Gaussian basis sets. J Comput Chem 29:225–232
23. Ledesma EB, Li C-Z, Nelson PF, Mackie JC (1998) Release of HCN, NH3, and HNCO from the thermal gas-phase cracking of coal pyrolysis tars. Energy Fuel 12:536–541
24. Yin F, Blumenfeld AL, Gruver V, Fripiat JJ (1997) NH3 as a probe molecule for NMR and IR study of zeolite catalyst acidity. J Phys Chem B 101:1824–1830
25. Li N, Ma X, Zha Q, Song C (2010) Analysis and comparison of nitrogen compounds in different liquid hydrocarbon streams derived from petroleum and coal. Energy Fuel 24:5539–5547
26. von Mühlen C, de Oliveira EC, Zini CA, Caramão EB, Marriott PJ (2010) Characterization of nitrogen-containing compounds in heavy gas oil petroleum fractions using comprehensive two-dimensional gas chromatography coupled to time-of-flight mass spectrometry. Energy Fuel 24:3572–3580
27. Dutriez T, Borras J, Courtiade M et al (2011) Challenge in the speciation of nitrogen-containing compounds in heavy petroleum fractions by high temperature comprehensive two-dimensional gas chromatography. J Chromatogr A 1218: 3190–3199
28. Mulliken RS (1955) Electronic population analysis on LCAO–MO molecular wave functions. I. J Chem Phys 23:1833–1840
29. Politzer P, Riley KE, Bulat FA, Murray JS (2012) Perspectives on halogen bonding and other σ-hole interactions: Lex parsimoniae (Occam's Razor). Comput Theor Chem 998:2–8